Check for updates

Received: 17 June 2021 | Accepted: 23 September 2021

DOI: 10.1002/pamm.202100098

Modeling the Mullins effect of rubbers used in constrained-layer damping applications

Alexander Jackstadt[1,*], **Felix Frölich**[1], **Kay Weidenmann**[2], and **Luise Kärger**[1]

[1] Karlsruhe Institute of Technology (KIT), Institute of Vehicle System Technology, Rintheimer Querallee 2, 76131 Karlsruhe, Germany

[2] University of Augsburg, Institute of Materials Resource Management, Am Technologiezentrum 8, 86159 Augsburg, Germany

The benefits of incorporating rubber interlayers in lightweight laminates, such as fiber-metal laminates, in order to compensate for their usually undesirable dynamic behavior have been studied in previous works [1, 2]. In such constrained-layer damping laminates, the rubber layers undergo large deformations due to their comparably low stiffness. This motivates the consideration of large strain phenomena commonly found in rubbers even when global laminate deformations are small such as in linear dynamic analysis. This work specifically addresses the cyclic softening of filled rubbers commonly known as the Mullins effect. As this effect significantly influences the elastic properties of the material, a change in the dynamic behavior of the laminate is to be expected. A constitutive model based on the work of Dorfmann and Ogden [3] for the prediction of the cyclic softening as well as residual strains upon unloading is presented in this study. Special consideration is given to the implementation of the model for use in a commercial implicit finite element solver by building on the work of Connolly et al. [4]. The model is validated against experimental data and compared to a current state-of-the-art model with regard to its predictive quality and computational efficiency. Furthermore, the experimental identification of material parameters for said model is addressed.

© 2021 The Authors. *Proceedings in Applied Mathematics & Mechanics* published by Wiley-VCH GmbH.

1 Introduction

Lightweight structures by nature feature comparably high stiffness with a low mass. This can lead to vibration and undesirable dynamic behavior. One passive mechanism used for the damping of these lightweight structures is the incorporation of viscoelastic damping layers in fiber-metal laminates (FMLs). The benefits of damping mechanism, named constrained-layer damping (CLD), have been shown by Liebig et al. [1] and Sessner et al. [2].

In general, filled rubbers are used as damping layers in CLD applications. With filled rubbers, however, the presence of cyclic softening is to be expected. [5] This cyclic softening effect has been the subject of numerous previous studies and is known as Mullins effect after the author of some directional works on this effect such as [6]. Although the Mullins effect is a large strain phenomenon, it should be considered in the modeling of CLD applications, as the strains observed in the damping layers exceed the global deformation of the laminate by far. Furthermore, deformations during manufacturing or assembly and possible static loads during operation can trigger the Mullins effect and thus affect the mechanical behavior of the damping layer.

This work deals with the experimental characterization and constitutive modeling of a rubber material used in CLD applications. Based on experimental findings, constitutive models are parameterized and investigated. Furthermore, the chosen pseudo-elastic model is formulated in principal stretches in order to be used in a commercial Finite Element Method (FEM) code.

2 Experimental characterization

The elastomer material investigated in this study is the filled ethylene propylene diene monomer (EPDM) rubber compound SAA9579-52 by Gummiwerk KRAIBURG GmbH & Co. KG. First, cyclic uniaxial tension tests are performed to characterize the occurrence of the Mullins effect. The specimens are extended to stretch levels $\lambda = \frac{L}{L_0} = 1.1; 1.2; 1.4; 1.8$. In order to mitigate viscoelastic effects, the strain rate is kept constant during loading and unloading. The specimens are unloaded until no tensile force is detected by the load cell. The strain on the specimen is measured contactless with a video extensometer.

The results of the cyclic tension test are shown in Fig. 1 in terms of nominal stress and strain for a strain rate of $\dot{\varepsilon} = 1.00 \times 10^{-3}\,\mathrm{s}^{-1}$. The curve clearly shows a softened behavior upon reloading up to the point of maximum strain. When this point is exceeded, the material's response follows the undamaged hyperelastic envelope. Furthermore, upon unloading to zero stress, significant residual strain is present.

* Corresponding author: e-mail alexander.jackstadt@kit.edu, phone +49 721 608 45365

This is an open access article under the terms of the Creative Commons Attribution License, which permits use, distribution and reproduction in any medium, provided the original work is properly cited.

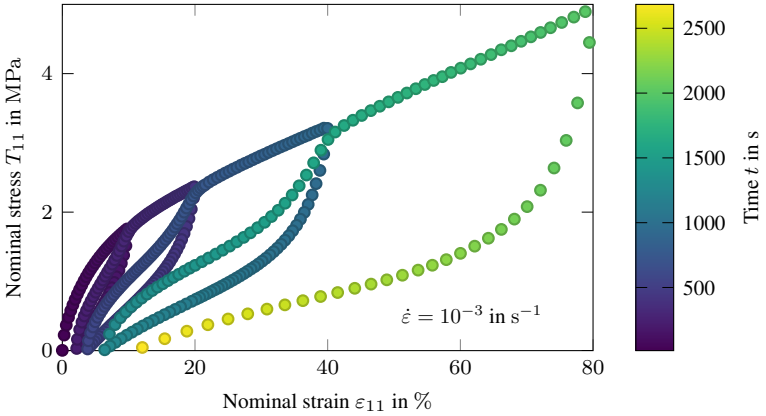

Fig. 1: Experimental results in uniaxial tension.

The softening (left) and residual strain (right) are quantitatively shown in Fig. 2 for two different strain rates. Although the overall secant modulus

$$E_n = \left.\frac{\Delta\sigma}{\Delta\varepsilon}\right|_{\varepsilon\in[0.2..5\%]} \tag{1}$$

is higher in case of the higher strain rate, the decrease is identical for both. The residual strain shows no difference between the two strain rates investigated.

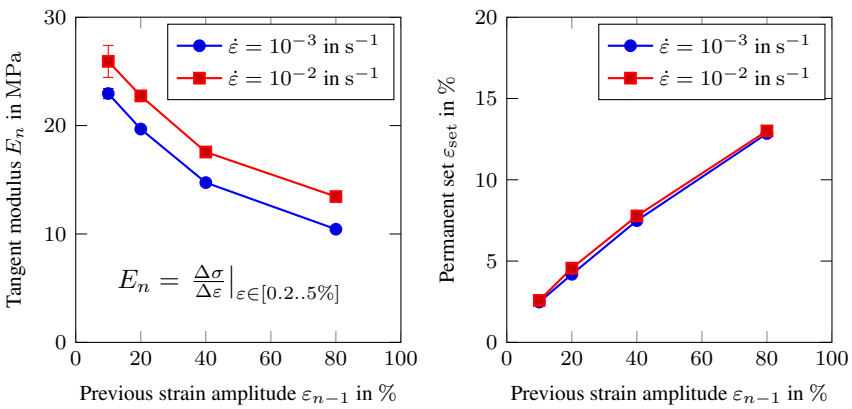

Fig. 2 Evaluation of uniaxial tension test results. The secant stiffness (left) is evaluated in a domain relevant for CLD application. The residual strain (right) is virtually identical for both strain rates.

3 Constitutive modeling

In this study, two constitutive models are investigated. The first one being the Ogden-Roxburgh model which is available in most commercial FEM codes. The less common Dorfmann-Ogden model is also considered here in order to better depict the experimental findings from Sec. 2.

3.1 Ogden-Roxburgh model

The Ogden-Roxburgh model, due to Ogden and Roxburgh [7], assumes a pseudo-elastic strain energy density of the form

$$W^{\text{dev}}(\lambda_i, \eta) = \eta \tilde{W}^{\text{dev}}(\lambda_i) + \Phi(\eta) \tag{2}$$

for incompressible materials. Eqn. (2) is formulated in dependence of the principal stretches λ_i. The purely hyperelastic deviatoric contribution to the strain energy density is denoted by $\tilde{W}^{\text{dev}}$. The softening of the material is accounted for by the damage parameter η. Energy dissipated due to the Mullins damage is represented in Eqn. (2) by a dissipation function $\Phi(\eta)$. For the given model, the damage parameter is formulated as

$$\eta = 1 - \frac{1}{r}\,\text{erf}\left(\frac{W^{\text{dev}}_{\max} - \tilde{W}^{\text{dev}}}{m + \beta W^{\text{dev}}_{\max}}\right). \tag{3}$$

The material parameters to be determined are r, m and β. The maximum deviatoric strain energy $W^{\text{dev}}_{\max}$ is a state variable depending on the load history of the material.

© 2021 The Authors. *Proceedings in Applied Mathematics & Mechanics* published by Wiley-VCH GmbH.

3.2 Dorfmann-Ogden model

The Dorfmann-Ogden model by Dorfmann and Ogden [3] is an extension of the previously described Ogden-Roxburgh model to account for residual strain as observed in Sec. 2. The strain energy density function in this case is formulated as

$$W^{\mathrm{dev}}\left(\lambda_i, \eta_1, \eta_2\right) = \eta_1 \tilde{W}^{\mathrm{dev}}\left(\lambda_i\right) + \left(1-\eta_2\right) N\left(\lambda_i\right) + \Phi\left(\eta_1, \eta_2\right). \tag{4}$$

The softening is described analogously to the Ogden-Roxburgh model by the parameter $\eta_1 = \eta$. Furthermore, a second damage parameter

$$\eta_2 = \tanh\left(\left(\frac{\tilde{W}^{\mathrm{dev}}}{W_{\max}^{\mathrm{dev}}}\right)^{\alpha\left(W_{\max}^{\mathrm{dev}}\right)}\right) \tanh\left(1\right)^{-1} \tag{5}$$

is introduced alongside the function $N\left(\lambda_i\right)$ to account for the contribution of the residual strain to the overall strain energy density. The function N is chosen as a modified strain energy function of a Neo-Hookean solid

$$N = \frac{1}{2}\left(\nu_1\left(\lambda_1^2-1\right) + \nu_2\left(\lambda_2^2-1\right) + \nu_3\left(\lambda_3^2-1\right)\right) \tag{6}$$

$$\nu_i\left(\lambda_{i,\max}\right) = \bar{a}\left(1 - \frac{1}{d}\tanh\left(\frac{\lambda_{i,\max}-1}{e}\right)\right) \tag{7}$$

following the suggestion in [3]. The exponent α is assumed to have the following dependence on $W_{\max}$:

$$\alpha\left(W_{\max}^{\mathrm{dev}}\right) = b + \bar{c} W_{\max}^{\mathrm{dev}} \tag{8}$$

The material parameters r, m, β, $\bar{a}$, b, $\bar{c}$, d and e need to be determined from experimental data. Parameters denoted with $\bar{()}$ refer to parameters, which in the original model [3] are expressed in dependence of the material's shear modulus. For reasons of brevity, the reader is referred to the original publications [3, 7] for a comprehensive deduction of the dissipation functions Φ.

3.3 Implementation

The two previously described models are implemented for the use in the commercial FEM code Abaqus using a user-material subroutine (UMAT). Since this requires the definition of the Jaumann rate of the Cauchy stress tensor $\mathbb{C}^J = \frac{1}{J}\frac{\partial\Delta(\boldsymbol{\sigma})}{\partial\Delta\boldsymbol{\varepsilon}}$ for which closed-form expressions are not straight forward to obtain, the framework of Connolly et al. [4] is adopted which allows the calculation of the required tensors for models defined in principal stretches. This procedure relies on the explicit calculation of principal stretches and principal directions in order to define the stress and elasticity tensors in the reference configuration before these are transformed to the current configuration. The required Jaumann rate of stress can then be derived. A comparison between a built-in implementation of the Ogden-Roxburgh model and the approach based on principal stretches is conducted in order to validate the implementation for pseudo-elasticity on the basis of an arbitrary material on a single finite element.

4 Results

Both models are fitted to the experimental data in Fig. 1 using the Differential Evolution algorithm due to Storm and Price [8]. Tabs. 1 and 2 list the parameters obtained. The corresponding model predictions are shown in Fig. 3. Both models depict well the loading and unloading curves. The Ogden-Roxburgh model, however, yields incorrect predictions close to the end of each unloading path since it does not capture the occurring residual strain. The Dorfmann-Ogden model on the other hand fits the curve well and yields good predictions for the residual strain and the secant modulus. Fig. 4 shows the comparison of the built-in Ogden-Roxburgh model in Abaqus and the implementation presented in this study for a single element test under uniaxial tension. The resulting loading and unloading curves are identical for both implementations. Furthermore, the automatically chosen time increments coincide in both cases, suggesting identical tangent matrices. A comparison of computation time is given in Tab. 3. It can be seen that the implementation presented here requires slightly more resources.

5 Conclusion

In this work, the experimental characterization of the Mullins effect in an rubber material used in CLD applications is presented for uniaxial loading. Two models, the Ogden-Roxburgh model and the Dorfmann-Ogden, model are parameterized in order to reproduce the experimental results. The Dormann-Ogden model yields good results as it is capable of capturing the residual strains observed in the experiment. Both pseudo-elastic models are implemented for the use in commercial FEM code Abaqus

 © 2021 The Authors. *Proceedings in Applied Mathematics & Mechanics* published by Wiley-VCH GmbH.

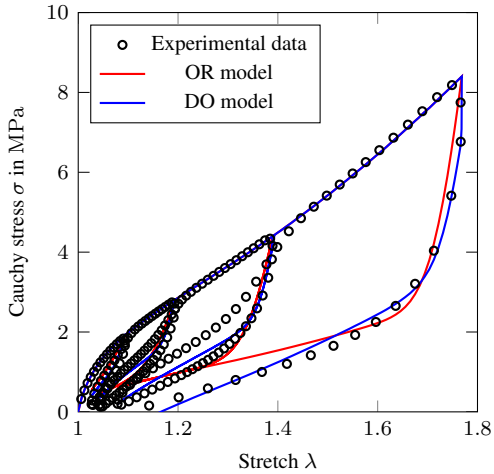

Fig. 3: Model predictions in comparison with experimental results in uniaxial tension.

Table 1: Parameters of the Ogden-Roxburgh model fitted to experimental data.

r	m	β
1.52	0.14	0.09

Table 2: Parameters of the Dorfmann-Ogden model fitted to experimental data.

r	m	β	$\bar{a}$ in MPa
2.56	2.23×10^{-2}	0.09	1.47
b in MPa	$\bar{c}$	d	e
1.00	8.61×10^{2}	6.64×10^{-1}	7.57×10^{-1}

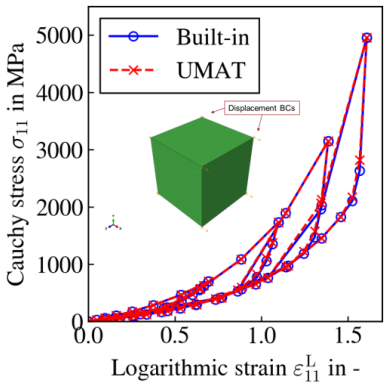

Fig. 4: Verification and comparison of the chosen implementation with the native Ogden-Roxburgh model available in Abaqus.

Table 3: Comparison of computational efficiency of the implemented model.

	Abaqus	UMAT
User time	3.00 s	3.30 s
System time	1.40 s	1.80 s
Total time	4.40 s	5.10 s

using the principal stretches approach previously published by Connolly et al. [4]. This implementation is equivalent to the native Abaqus implementation but requires slightly more resources. Future studies will involve further experiments in order to characterize the Mullins effect under different loading conditions, such as pure shear. Furthermore, the models will be extended to represent viscoelastic effects and dissipation present in the CLD mechanism.

Acknowledgements This work is funded by the Deutsche Forschungsgemeinschaft (DFG, German Research Foundation) SPP1897 "Calm, Smooth, Smart – Novel approaches for influencing vibrations by means of deliberately introduced dissipation", project KA 4224/3-2 and WE 4273/16-2, grant no. 314969583, "HyCEML – Hybrid CFRP/elastomer/metal laminates containing elastomeric interfaces for deliberate dissipation" (Karlsruhe Institute of Technology). The work is also part of the Young Investigator Group (YIG) "Green Mobility", generously funded by the Vector Stiftung. Furthermore, the authors would like to acknowledge Gummiwerk KRAIBURG GmbH & Co. KG for providing the elastomer material. Open access funding enabled and organized by Projekt DEAL.

References

[1] W. V. Liebig, V. Sessner, K. A. Weidenmann, and L. Kärger, Composite Structures **202**, 1109–1113 (2018).
[2] V. Sessner, A. Jackstadt, W. V. Liebig, L. Kärger, and K. A. Weidenmann, Journal of Composites Science **3**(1), 3 (2019).
[3] A. Dorfmann and R. W. Ogden, International Journal of Solids and Structures **41**(7), 1855–1878 (2004).
[4] S. J. Connolly, D. Mackenzie, and Y. Gorash, Computational Mechanics **64**(5), 1273–1288 (2019).
[5] J. Diani, B. Fayolle, and P. Gilormini, European Polymer Journal **45**(3), 601–612 (2009).
[6] L. Mullins, Rubber Chem. Technol. **42**(1), 339–362 (1969).
[7] R. W. Ogden and D. G. Roxburgh, Proc. R. Soc. A Math. Phys. Eng. Sci. **455**(1988), 2861–2877 (1999).
[8] R. Storn and K. Price, Journal of Global Optimization **11**(4), 341–359 (1997).

© 2021 The Authors. *Proceedings in Applied Mathematics & Mechanics* published by Wiley-VCH GmbH.